Cancer Immunology, Immunotherapy (2025) 74:20
https://doi.org/10.1007/s00262-024-03847-7

RESEARCH

Loop33 × 123 CAR-T targeting CD33 and CD123 against immune escape in acute myeloid leukemia

Haotian Ma[1,2] · Zhifeng Yan[1,2] · Runxia Gu[1,2] · Yingxi Xu[1,2] · Shaowei Qiu[1,2] · Haiyan Xing[1,2] · Kejing Tang[1,2] · Zheng Tian[1,2] · Qing Rao[1,2] · Min Wang[1,2] · Jianxiang Wang[1,2]

Received: 30 June 2024 / Accepted: 24 September 2024

Abstract

Background Immunotherapy, such as chimeric antigen receptor T (CAR-T) cells targeting CD33 or CD123, has been well developed over the past decade for the treatment of acute myeloid leukemia (AML). However, the inability to sustain tumor-free survival and the possibility of relapse due to antigen loss have raised concerns. A dual targeting of CD33 and CD123 is needed for better outcomes.

Methods Based on our previously constructed CD33 and CD123 monovalent CAR-T, Loop33 × 123 and Loop123 × 33 CAR-T were constructed with molecular cloning techniques. All CAR-T cells were generated by lentivirus transduction of T cells from healthy donors. Phenotype detection was evaluated on day 7 concerning activation, exhaustion, and subtype proportions. Coculture killing assays were conducted using various AML cell lines and primary AML cells. Degranulation and cytokine secretion levels were detected by flow cytometry. Cell-derived xenograft models were established using wild-type Molm 13 cell lines, or a mixture of Molm 13-KO33 and Molm 13-KO123 cells as an ideal model of immune escape. By monitoring body weight and survival of tumor-bearing mice, Loop33 × 123 and Loop123 × 33 CAR-T cells were further assessed for their efficacy in vivo.

Results In vitro study, our results demonstrated that Loop33 × 123 CAR-T cells could efficiently eliminate AML cell lines and primary AML cells with elevated degranulation and cytokine secretion levels. Compared with our previously constructed monovalent CD33 or CD123 CAR-T cells, Loop33 × 123 CAR-T cells showed superior advantages in an immune escape model. In vivo studies further confirmed that Loop33 × 123 CAR-T cells could effectively prolong the survival of mice without significant toxicity. However, Loop123 × 33 CAR-T cells failed to show the same effects. Furthermore, Loop33 × 123 CAR-T cells efficiently circumvented potential immune escape, a challenge where monovalent CAR-T cells failed.

Conclusions Loop33 × 123 CAR-T targeting CD33 and CD123 could efficiently eliminate AML cells and prolong survival of tumor-bearing mice, while addressing the issue of immune escape.

Keywords AML · Chimeric antigen receptor · CD33 · CD123

Introduction

Acute myeloid leukemia (AML) stands as the most prevalent form of leukemia among adults, with approximately 20,380 new cases diagnosed and 11,310 deaths reported in the USA in 2023 [1]. Despite notable advancements in conventional AML therapies such as cytarabine and anthracycline, as well as mutation-specific targeted therapies like FLT3, IDH1, IDH2, and RAS inhibitors, their curative efficacy remains below approximately 50% [2].

Chimeric antigen receptor T (CAR-T) cells, comprising synthetic polypeptides with extracellular, hinge, transmembrane, and co-stimulatory domains, have emerged as

✉ Min Wang
wangjxm@ihcams.ac.cn

✉ Jianxiang Wang
wangjx@ihcams.ac.cn

[1] State Key Laboratory of Experimental Hematology, National Clinical Research Center for Blood Diseases, Tianjin Key Laboratory of Cell Therapy for Blood Diseases, Haihe Laboratory of Cell Ecosystem, Institute of Hematology and Blood Diseases Hospital, Chinese Academy of Medical Sciences and Peking Union Medical College, 288 Nanjing Road, Tianjin 300020, China

[2] Tianjin Institutes of Health Science, Tianjin 301617, China

Published online: 13 November 2024

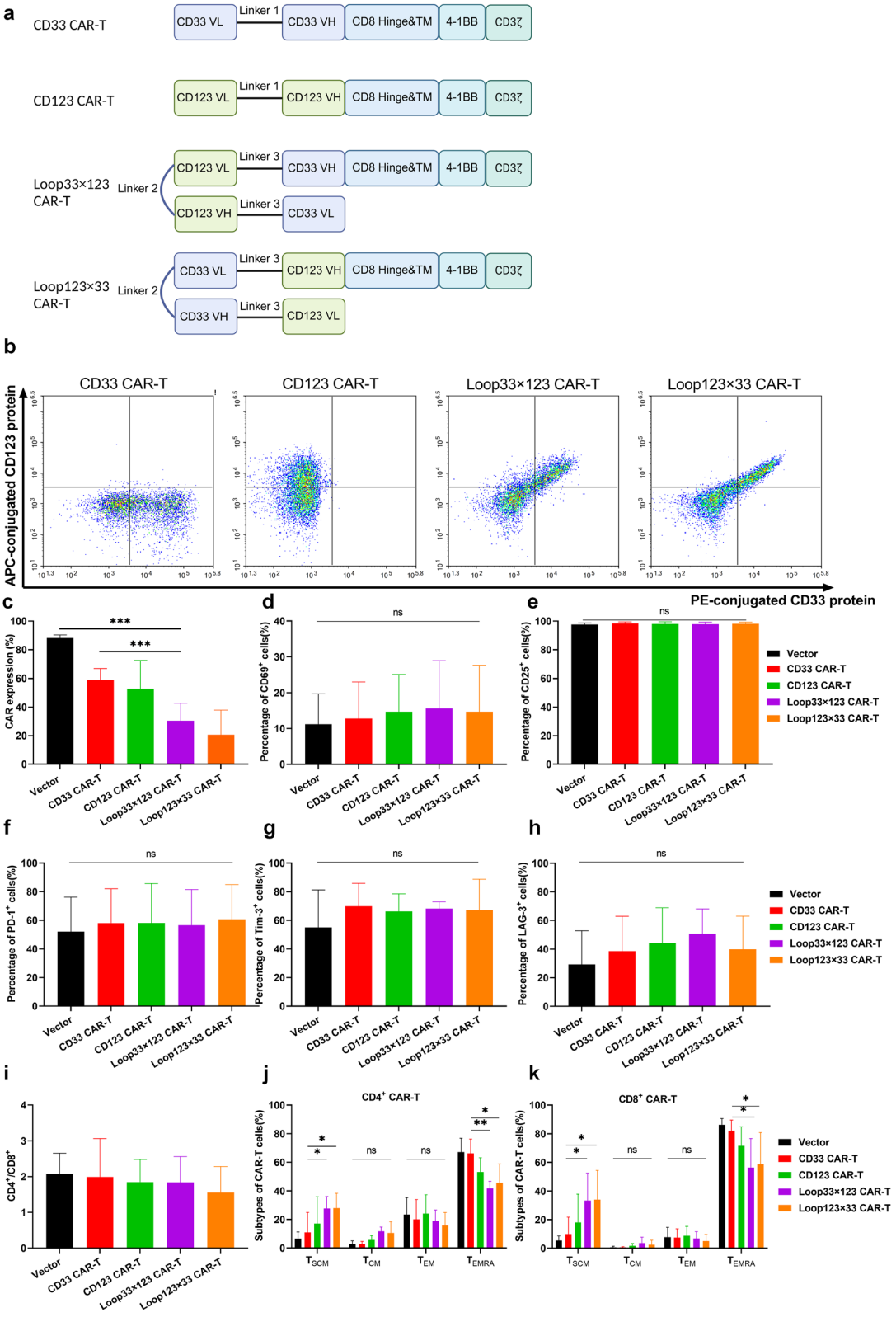

promising therapeutic methods for hematological malignancies [3]. CAR-T cells targeting CD19 have demonstrated exciting antitumor effects in B cell malignancies over the past decade [4], but its application in AML has been relatively limited due to the lack of a universal target antigen [5].

◂**Fig. 1** Construction of Loop33 × 123 and Loop123 × 33 CAR-T cells targeting both CD33 and CD123 **a** Schematic display of CD33 CAR-T, CD123 CAR-T, Loop33 × 123 CAR-T, and Loop123 × 33 CAR-T. **b** Representative flow cytometry diagram showed that Loop CAR-T could recognize CD33 and CD123 proteins. **c** Flow cytometry detection of CAR expression on day 7. **d**, **e** Flow cytometry detection of activation markers CD69 and CD25 on day 7. **F**–**h** Flow cytometry detection of exhaustion markers PD-1, Tim-3, and LAG-3 on day 7. **i** Flow cytometry detection pf $CD4^+/CD8^+$ ratio on day 7. **j**, **k** Flow cytometry detection of stem cell memory cells (T_{SCM}), central memory cells (T_{CM}), effector memory cells (T_{EM}), and terminal differentiation effector cells (T_{EMRA}) in $CD4^+$ and $CD8^+$ cells, respectively. *, $p < 0.05$; **, $p < 0.01$; ns, no significance

CD33 is a transmembrane sialic acid-binding immunoglobulin-type lectin (SIGLEC) receptor expressed on the surface of AML blasts, mature myeloid cells and hematopoietic progenitor cells [6, 7]. In addition, it was implied that CD33-directed therapy could potentially eradicate malignant stem or progenitor cells [8, 9]. However, with limited clinical outcomes, patients treated with gentuzumab ozogamicin (GO) or CD33 CAR-T alone relapsed with $CD33^-$ or $CD33^+$ AML [10–12], implying that an additional target antigen could help eliminate leukemic cells.

Besides CD33, CD123 serves as an ideal target. It is a glycoprotein of the α subunit of the interleukin-3 receptor (IL-3αA) and is expressed on AML blasts with association with high risks [13–15]. More importantly, it is highly expressed on $CD34^+CD38^-$ leukemic stem cells (LSCs) and is absent from or minimally expressed on normal hematopoietic stem cells (HSCs) [16, 17]. A sophisticated study had revealed that the simultaneous presence of both antigens was observed in 69.5% of AML patients, but still 9.4% of AML patients expressed CD123 without concomitant CD33 expression [18]. While individual immunotherapy targeting CD33 or CD123 alone has been carefully validated in certain preclinical and clinical studies [19–23], the potential of antigen loss has also been noted [24, 25], necessitating further exploitation into a dual targeting strategy.

Common dual targeting strategies concerning CAR-T cell therapy include sequential infusion of different CAR-T cells [26, 27], tandem CAR-T [28, 29], compound CAR-T [30, 31], and loop CAR-T [32]. In addition, a delicate study had confirmed that loop CAR-T demonstrated stronger killing effects and longer persistence in vivo than tandem CAR-T [32].

In this study, we demonstrated a novel strategy of CAR-T cells targeting both CD33 and CD123 by using a loop construct. We compared them with the previously constructed monovalent CD33 CAR-T [33] and CD123 CAR-T [31, 33] and demonstrated that loop CAR-T cells could effectively eradicate tumor cells in an immune escape system both in vitro and in vivo.

Results

Construction of Loop33 × 123 and Loop123 × 33 *CAR*-T cells targeting both CD33 and CD123

We utilized the anti-CD33 single chain variable fragment (scFv) and anti-CD123 scFv to generate the antigen binding site of the bispecific chimeric antigen receptors (CARs), incorporating the CD8 hinge and transmembrane domain, as well as the 4-1BB co-stimulatory domain. Altering the light and heavy chains of the scFv for optimization, they were termed Loop33 × 123 CAR-T and Loop123 × 33 CAR-T, respectively (Fig. 1a). All CAR-T cells were produced by transduction of primary peripheral blood T cells from healthy donors with lentivirus. Vector-transduced cells (Vector-T) without extracellular antigen-binding domains were served as controls. All CAR-T cells demonstrated steady and persistent expression of CARs throughout the in vitro culture, and their infection efficiency was assessed on day 7. Besides Fab expression, the bispecific Loop CAR-T cells could recognize both CD33 and CD123 florescent proteins, whereas monovalent CAR-T cells could only bind either of proteins (Fig. 1b, c). Loop33 × 123 CAR-T and Loop123 × 33 CAR-T cells showed a relatively lower CAR expression [(34.05 ± 12.18)% and (26.62 ± 15.19)%, respectively, $p < 0.001$] on day 7 possibly due to larger recognition domains than those of monovalent CAR-T cells [(58.48 ± 9.17)% and (49.65 ± 22.90)%, respectively, $p < 0.001$].

To determine whether different constructs could affect the phenotypes of CAR-T cells, we analyzed cell surface markers related to activation, exhaustion, and subtypes on day 7 of culture. All CAR-T cells expressed relatively similar levels of CD69, CD25, PD-1, Tim-3, and LAG-3, indicating that Loop CAR-T cells were activated to the same level as monovalent CAR-T cells without showing higher markers of exhaustion (Fig. 1d–h). In the subtype analysis, the memory markers CD45RA and CCR7 were detected, and CAR-T cells were subsequently categorized into four groups: stem cell memory cells (T_{SCM}), central memory cells (T_{CM}), effector memory cells (T_{EM}), and terminally differentiated effector cells (T_{EMRA}). While the $CD4^+/CD8^+$ ratio remained unchanged across all groups (Fig. 1i), it was noteworthy that Loop33 × 123 and Loop123 × 33 CAR-T cells had a higher proportions of $CD4^+$ T_{SCM} cells [(27.64 ± 8.49)% and (28.01 ± 10.27)%, respectively, $p < 0.05$] and $CD8^+$ T_{SCM} [(33.25 ± 19.23)% and (33.93 ± 20.44)%, respectively, $p < 0.05$], and lower proportions of T_{EMRA} cells compared to that of Vector-T and monovalent CAR-T cells (Fig. 1j, k). This phenotypic distribution is widely speculated to contribute to reduced exhaustion and increased potency in proliferation and function.

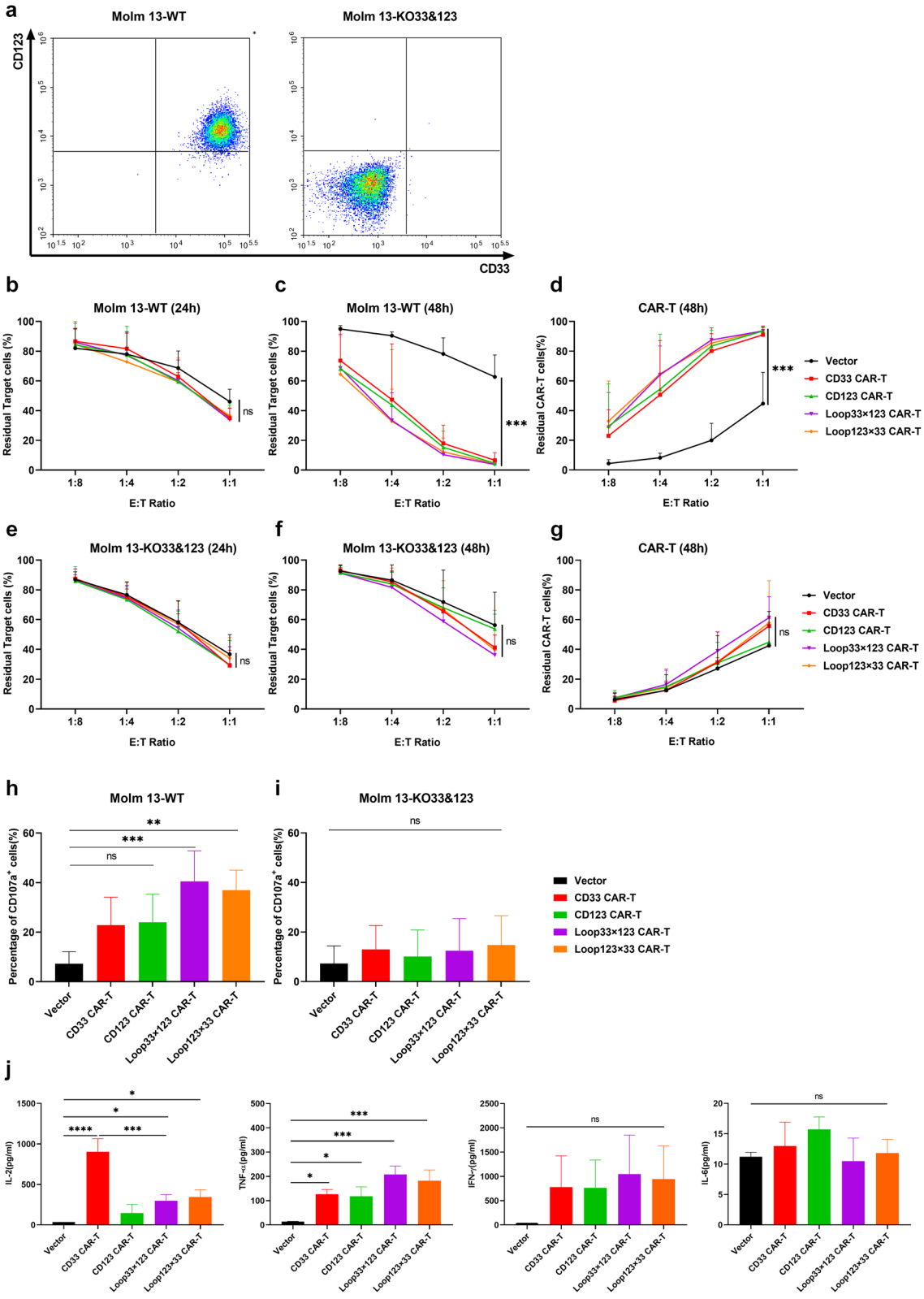
a
Molm 13-WT
Molm 13-KO33&123
CD123
CD33
b
Molm 13-WT (24h)
Residual Target cells (%)
E:T Ratio
ns
c
Molm 13-WT (48h)
***
d
CAR-T (48h)
Residual CAR-T cells(%)
Vector
CD33 CAR-T
CD123 CAR-T
Loop33×123 CAR-T
Loop123×33 CAR-T
e
Molm 13-KO33&123 (24h)
f
Molm 13-KO33&123 (48h)
g
CAR-T (48h)
h
Molm 13-WT
Percentage of CD107a+ cells(%)
**
***
ns
i
Molm 13-KO33&123
j
IL-2(pg/ml)
TNF-α(pg/ml)
IFN-γ(pg/ml)
IL-6(pg/ml)
*
****

◂**Fig. 2** Loop CAR-T efficiently eliminated AML cell lines than monovalent CAR-T **a** FCM shows CD33 and CD123 expression of Molm 13-WT and Molm 13-KO33&123. **b**–**g** Residual target cells and CAR-T cells at 24 and 48 h after Vector-T or CAR-T cells were cocultured with Molm 13-WT cells or Molm 13-KO33&123 at various E:T ratios. **h**, **i** Degranulation of Vector-T or CAR-T cells defined as $CD107a^+$ cells after coculturing with Molm 13-WT cells or Molm 13-KO33&123 for 6 h. **j** IL-2, IL-6, TNF-α, and IFN-γ secretion of Vector-T or CAR-T cells after coculturing with Molm 13-WT cells for 24 h. *, $p<0.05$; **, $p<0.01$; ***, $p<0.001$; ****, $p<0.0001$; ns, no significance

Loop *CAR*-T efficiently eliminated AML cell lines than monovalent *CAR*-T

While the wild-type AML cell line Molm 13 (Molm 13-WT) was simultaneously positive for CD33 and CD123, we used CRISPR-Cas9 technology to knock out both markers to establish the Molm13-KO33&123 as a negative control (Fig. 2a). The expression of CARs was adjusted to 30% with untransduced T cells before coculture on day 7. After coculturing Vector-T or CAR-T cells with Molm 13-WT or Molm 13-KO33&123, residual cells were determined by flow cytometry (FCM) at indicated time points, including $CD3^+$ T cells, $CD3^-$ $CD33^+$ Molm 13-WT, and $CD3^-$ Molm 13-KO33&123. Significant lysis of the tumor cells by Loop CAR-T cells was observed even at a low effector-to-target (E:T) ratio of 1:8 at 48 h, and Loop CAR-T cells proliferated robustly compared to that of Vector-T cells (Fig. 2b–d). In contrast, Loop CAR-T cells did not exhibit nonspecific cytotoxicity toward Molm13-KO33&123 cells (Fig. 2e–g). The expression of CD107a on the surface of T cells, which served as a marker of degranulation and early activation, was detected 6 h after coculturing at a 1:1 E:T ratio. Notably, Loop33 × 123 CAR-T cells demonstrated significantly higher expression of CD107a [$(40.45 \pm 12.35)\%$, $p<0.001$], indicating a more intense degranulation effect at early stages (Fig. 2h). In contrast, no significant increase in CD107a expression was observed when Loop33 × 123 CAR-T cells cocultured with Molm13-KO33&123, validating their safety in the absence of corresponding antigens (Fig. 2i).

Supernatants were collected after 24 h of coculturing, and cytokines were detected by cytometric bead array (CBA). Vector-T cells and all CAR-T cells did not show differences in interleukin-6 (IL-6) secretion. CD33 CAR-T cells significantly secreted more interleukin-2 (IL-2) than that of Loop33 × 123 CAR-T cells [(902.1 ± 162.0) pg/ml vs. (298.1 ± 76.4) pg/ml, $p<0.001$], whereas the latter secreted more tumor necrosis factor α (TNF-α) and interferon γ (IFN-γ), though not statistically significant (Fig. 2j).

To further validate the efficiency of Loop CAR-T cells, we performed experiments with another AML cell line MV4-11 cells, which were also simultaneously positive for CD33 and CD123 (Supplementary Fig. S1a). Similarly, Loop CAR-T cells demonstrated strong and persistent cytotoxicity toward tumor cells, elevated degranulation, and cytokine secretion ability (Supplementary Fig. 1b–h).

Our in vitro killing assays revealed that Loop33 × 123 CAR-T and Loop123 × 33 CAR-T could significantly target AML cell lines with minimal off-target effects and decreased IL-2 secretion compared to that of monovalent CAR-T cells.

Loop *CAR*-T cells could effectively eliminate patients' primary AML cells in vitro

Primary bone marrow mononuclear cells (BMMNCs) were randomly collected from six AML patients for further investigation and evaluation of Loop CAR-T cells, and the surface expression of CD33 and CD123 was detected before the coculture (Fig. 3a, b, Table 1). At 48 h, all CAR-T cells could efficiently eradicate primary tumor cells compared to Vector-T cells ($p<0.05$), though tumor lysis efficiency varied vastly within each group due to patient's heterogeneity (Fig. 3c). Loop CAR-T cells showed elevated levels of CD107a and cytokine secretion ($p<0.001$), whereas no significant differences were observed within four CAR-T groups (Fig. 3d, e). CD123 CAR-T demonstrated a slightly higher IL-2 secretion than that of CD33 CAR-T [(2727.4 ± 703.1) pg/ml vs (1676.2 ± 524.2) pg/ml, $p=0.107$].

To provide deeper validity and broader applicability of this study, we screened samples from newly diagnosed M1, M3, and M4 AML subtypes with high expression of CD123 and CD33 (Supplementary Fig. 2a, Supplementary Table 1). While Vector-T showed minimal cytotoxicity toward primary cells, all CAR-T showed comparable elimination of tumor cells, elevated degranulation, and abundant cytokine secretion.

Loop33 × 123 *CAR*-T cells could significantly prolong survival in tumor bearing mice

To evaluate Loop CAR-T cells in vivo, we established a cell derived xenograft (CDX) mouse model with Molm 13-WT cells transduced with luciferase. The NOD. CB17-$Prkdc^{scid}Il2rg^{tm1Bcgen}$/Bcgen (B-NDG) mice were injected with 1×10^6 Molm 13-WT cells through the tail vein on day −3, and were randomly grouped by weight and total bioluminescence signal intensity on day 0. On day 1, 5×10^6 Vector-T or CAR-T cells were intravenously injected (Fig. 4a). Body weight and bioluminescence intensity were monitored weekly. Weight loss was not observed in all CAR-T groups, compared to drastic weight loss in mice treated with Vector-T cells (Fig. 4c). This strongly indicated that tumor-bearing mice treated with CAR-T cells showed rapid disease control and did not undergo life-threatening side effects. The body weight of the mice treated with Vector-T cells was significantly

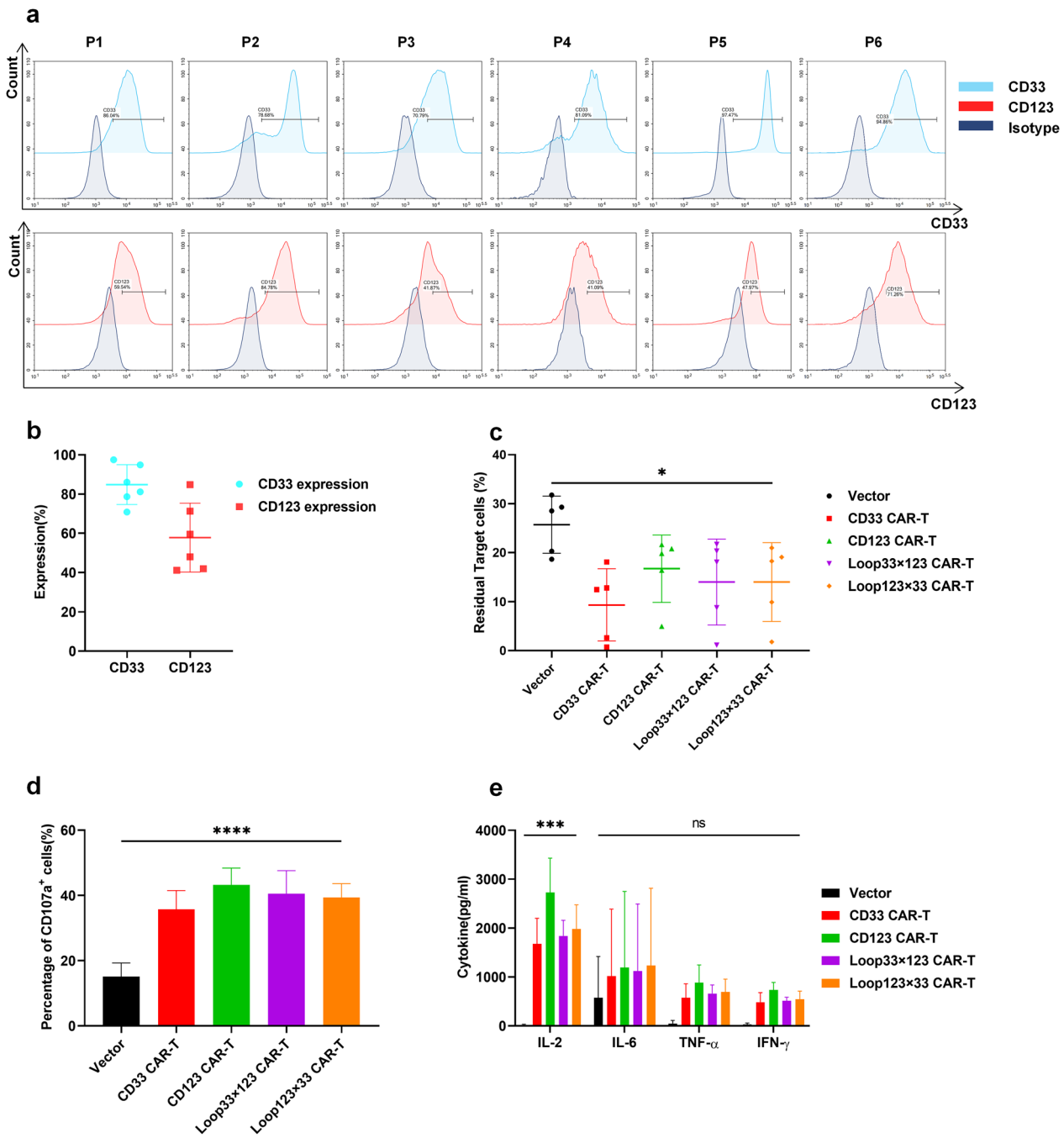

Fig. 3 Loop CAR-T cells could effectively eliminate patients' primary AML cells in vitro **a** FCM shows CD33 and CD123 expression of six AML patients primary cells. **b** Summary plot of CD33 and CD123 expression of primary cells. **c** Percentage of residual target cells at 48 h after coculturing at E:T ratio of 1:1. **d** Degranulation of Vector-T or CAR-T cells after coculturing with primary cells. **e** IL-2, IL-6, TNF-α, and IFN-γ secretion of Vector-T or CAR-T cells after coculturing with primary cells for 24 h. *, $p<0.05$; **, $p<0.01$; ***, $p<0.001$; ****, $p<0.0001$; ns, no significance

decreased on day 14 due to the rapid progression of the disease, confirmed by a significant increase in bioluminescence signal intensity compared to mice treated with CAR-T cells (Fig. 4b, d).

Although CAR-T cells successfully prolonged the survival of all mice, significant differences in bioluminescence signal intensity and survival time were observed among four groups. On day 21, mice treated with CD123 CAR-T and Loop123×33 CAR-T cells had significantly higher levels of tumor burden, as evidenced by widespread tumor cells in organs and higher bioluminescence signal intensity (Fig. 4b, d). The median survival time for these two groups

Table 1 Patient information

Patient ID	Disease	Sample Type	CD33 expression	CD123 expression
P1	AML M5	BM	86.04%	59.54%
P2	AML M5	BM	94.86%	71.26%
P3	AML M2	BM	70.79%	41.87%
P4	AML M5	BM	97.47%	47.97%
P5	AML M5	BM	78.68%	84.78%
P6	AML M2b	BM	81.09%	41.09%

was 19.5 and 24 days, respectively, which was significantly longer than that of the Vector-T group of merely 14 days ($p < 0.001$). In sharp contrast, mice treated with CD33 CAR-T and Loop33×123 CAR-T cells demonstrated restrained tumor spreading and significantly lower bioluminescence signal intensity on day 21. The median survival of the CD33 CAR-T and Loop33×123 groups was 39 and 47.5 days, respectively, which was significantly longer than those treated with CD123 CAR-T and Loop123×33 CAR-T cells ($p < 0.01$) (Fig. 4e).

We collected blood serum from all mice in the four treatment groups on day 15 for cytokine detection and tried to explore the possible mechanisms behind the early loss of control in the CD123 CAR-T and Loop123×33 CAR-T groups. However, minimal differences were observed in vital cytokine levels, including IL-2, IL-6, TNF-α, and IFN-γ (Fig. 4f). A slight increase in IFN-γ in the CD33 CAR-T group [(100.3 ± 49.5) pg/ml, $p < 0.05$] and Loop123×33 CAR-T group [(101.4 ± 117.9) pg/ml, $p < 0.05$] was observed compared to that of the Loop33×123 group, which was not considered to be the dominant reason for the failure of Loop123×33 to control tumor progression in this model.

Overall, the in vivo results indicated that Loop33×123 CAR-T cells could significantly prolong survival in tumor-bearing mice without noticeable side effects. However, Loop123×33 failed to show similar efficacy.

Loop33×123 *CAR*-T cells were efficient to avoid immune escape in vitro and in vivo

To simulate possible antigen loss in cells co-expressing CD33 and CD123, we knocked out CD33 or CD123 in Molm 13-WT cells to establish Molm 13-KO33 and Molm 13-KO123 (Fig. 5a). After coculturing, residual cells were determined by FCM, including $CD3^+$ T cells, $CD3^-$ $CD33^-$ $CD123^+$ Molm 13-KO33, and $CD3^-$ $CD33^+$ $CD123^-$ Molm 13-KO123.

CAR-T cells were cocultured with Molm 13-KO33 or Molm 13-KO123, respectively, at indicated E:T ratios. Tumor cells were not eliminated at 24 h but were drastically eradicated at 48 h. As expected, CD33 CAR-T cells failed to target Molm 13-KO33 cells ($p < 0.01$), as CD123 CAR-T cells failed to target Molm 13-KO123 cells ($p < 0.001$). Significant differences in the proliferation of Vector-T cells and CAR-T cells were not observed at 48 h, though CD33 CAR-T and CD123 CAR-T cells showed minimal proliferation when cocultured with targets without corresponding antigens, indicating that monovalent CAR-T cells were less efficient when tumor cells progress with antigen loss (Fig. 5b–g).

We then mixed Molm 13-KO33 and Molm 13-KO123 cells in a 1:1 ratio to serve as target cells. All CAR-T cells induced significant and substantial cytotoxicity against the tumor cells compared to that of Vector-T cells ($p < 0.05$) (Fig. 5h). However, there was a notable difference in the proportion of Molm 13-KO33 and Molm 13-KO123 within the residual tumor cells (Fig. 5i, j). CD33 CAR-T cells induced specific cytotoxicity against Molm 13-KO123, while sparing almost all Molm 13-KO33 cells within the system. Both Loop33×123 and Loop123×33 CAR-T cells, in sharp contrast, exhibited significant cytotoxicity toward either group of tumor cells without any biased effects. To our surprise, CD123 CAR-T cells also showed unbiased cytotoxicity, eliminating Molm 13-KO33 and Molm 13-KO123 cells equally. One possible reason for this phenomenon could be antigen spreading. Therefore, we cocultured CD123 CAR-T or Vector-T cells with Molm 13-KO33 (Supplementary Fig. 3a). After 24 h, we found that CD123 CAR-T eradicated Molm 13-KO33 cells (Supplementary Fig. 3b). We then sorted out CD123 CAR-T or Vector-T cells in this system and cocultured them with Molm 13-KO123 cells, respectively. Surprisingly, CD123 CAR-T showed cytotoxicity toward Molm 13-KO123 cells after coculturing with Molm 13-KO33 cells (Supplementary Fig. 3c).

We then assessed degranulation levels and cytokine secretion in all groups (Fig. 5 k, l). CD33 CAR-T and CD123 CAR-T cells failed to degranulate when challenged with cells lacking the corresponding antigens. In contrast, Loop33×123 CAR-T cells demonstrated the highest degranulation levels and cytokine secretion when cocultured with either type of tumor cells, indicating that Loop33×123 CAR-T cells could be robustly activated even when CD33 or CD123 was missing, and could function better than monovalent CAR-T cells. In addition, all CAR-T cells induced more cytokine secretion compared to that of Vector-T cells against the mixture of Molm 13-KO33 and Molm 13-KO123, especially in IFN-γ (Fig. 5l).

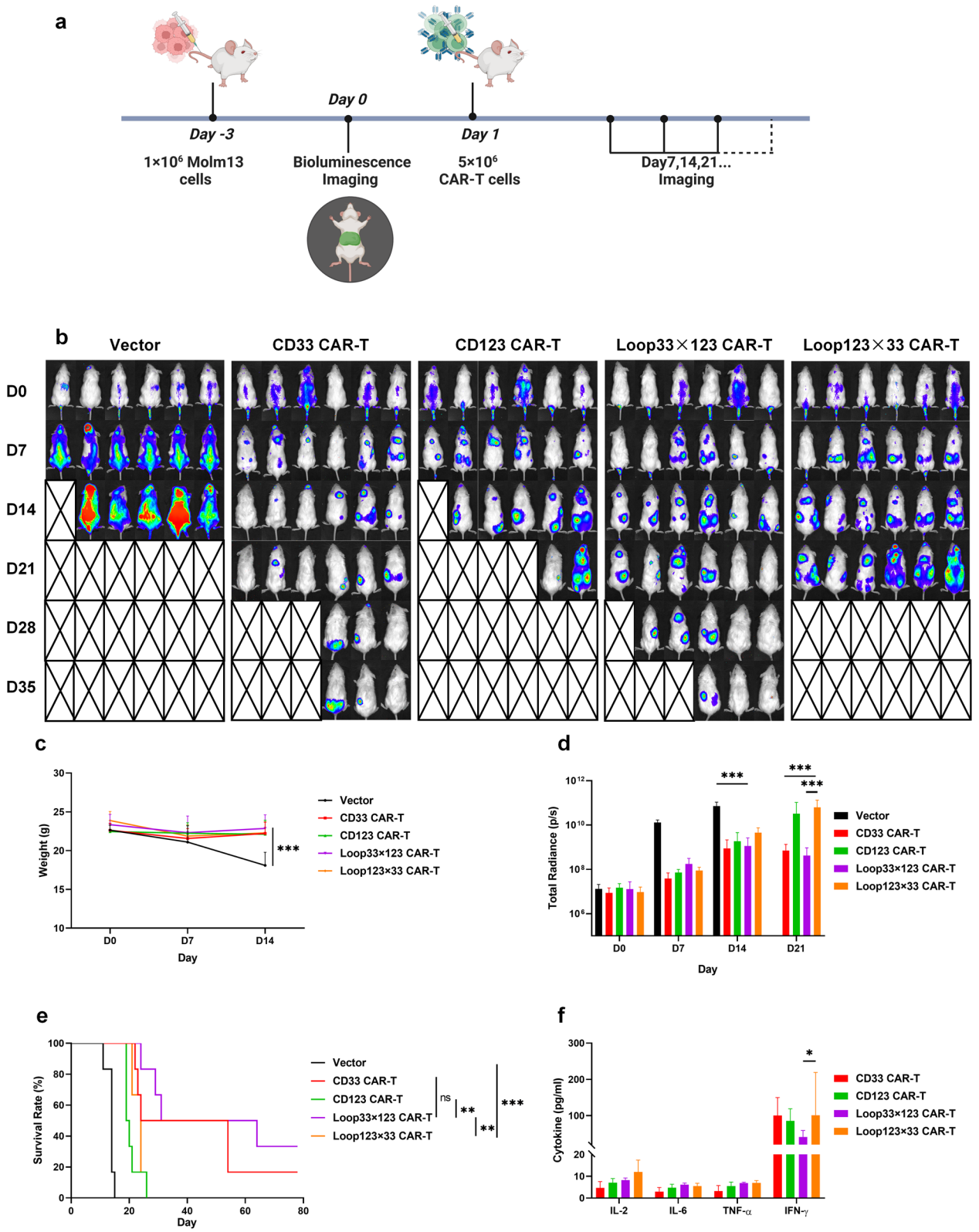

Fig. 4 Loop33×123 CAR-T cells could significantly prolong survival in tumor bearing NSG mice **a** The experimental regimen of the B-NDG-CDX model. **b** Bioluminescence imaging showing tumor burden over time (n = 6). **c** The body weight of each group was measured after treatment with Vector-T or CAR-T cells. **d** Statistical analysis of the bioluminescence intensity. **e** Kaplan–Meier survival curves for each group. (f) Cytokine levels of mice blood serum of each group on day 15. *, $p < 0.05$; **, $p < 0.01$; ***, $p < 0.001$; ****, $p < 0.0001$; ns, no significance

We further explored the potency of Loop CAR-T against this immune evasion model in vivo. The B-NDG mice were injected with 0.5×10^6 Molm 13-KO33 cells and 0.5×10^6 Molm 13-KO123 cells through the tail vein on day −3 and then were randomly grouped by weight and total bioluminescence signal intensity on day 0. On day 1, 5×10^6 Vector-T or CAR-T cells were intravenously injected (Fig. 6a). Body weight and bioluminescence intensity were monitored weekly (Fig. 6b). The Loop33×123 CAR-T group did not undergo noticeable weight loss for the first two weeks, whereas mice in all other groups showed considerable weight loss, possibly due to disease progression (Fig. 6c).

While mice treated with Vector-T cells had a poor median survival of 13 days, mice treated with CD33 CAR-T cells, CD123 CAR-T, or Loop123×33 CAR-T cells showed only a slight prolongation of survival to 15 days. In contrast, the Loop33×123 CAR-T group had a profound survival of 51.5 days ($p<0.001$) (Fig. 6d). Although bioluminescence signal intensity suggested that the other three treatment groups had lower tumor burdens on day 14 than that of the Vector-T group, these mice failed to show disease control and died in the following week (Fig. 6e).

In conclusion, Loop33×123 CAR-T cells demonstrated strong efficiency in preventing immune evasion and escape in our model, whereas other CAR-T cells failed.

Discussion

CD33 was reported to be positive in blasts in more than 85% of AML patients [34]. It was reported that targeting CD33 seemed to be harmless to normal hematopoietic stem cells [35], making it an ideal target for AML treatment. The anti-CD33 antibody–drug compound (ADC) gemtuzumab ozogamicin (GO; Mylotarg) demonstrated a beneficial outcome and a great example of targeting CD33 [36, 37]. CD123 was another well-studied target. In a recent clinical trial, IMGN632, another ADC targeting CD123 was evaluated for its efficacy [38]. Beside ADC, bispecific antibodies were also a promising way to activate host T cells for tumor elimination [35, 39]. In this study, we sought for a strategy for complete elimination of tumor blasts with bispecific CAR-T therapy.

While CAR-T cell therapy targeting CD33 or CD123 demonstrated considerable efficacy against AML in the past decade [40–42], several setbacks such as limited cytotoxicity or immune escape were observed. It was reported that patients could relapse with $CD33^+$ AML after receiving sufficient amount of GO [43]. In addition, a patient received CD33 CAR-T in a clinical trial subsequently died with consistent detectable $CD33^+$ tumor cells in blood and bone marrow [44]. In order to address these existing issues, we chose to design a bispecific CAR-T that could simultaneously target CD33 and CD123.

Our recent work showed that a compound CD33×CD123 CAR-T therapy was efficient both in vitro and in vivo with minimal side effects [31]. In addition, our previous work demonstrated efficient eradication of tumor cells by CAR-T cells with a loop construct or a tandem construct [32]. In this specific scenario, we found out that tandem33×123 or tandem123×33 showed lower cytotoxicity and unsatisfying CAR expression (data not shown). To achieve higher infection efficiency and better expression of the CAR molecules, we further developed Loop CAR-T cells and examined their efficacy, including their phenotypes, cytotoxicity, and cytokine secretion ability. As the results showed, Loop33×123 CAR-T could efficiently target CD33 and CD123 simultaneously both in vitro and in vivo without notable side effects, and it was significantly efficient against possible antigen loss compared to monovalent CAR-T.

It was implied that CAR-T cells without antigen stimulation predominantly exhibit a T_{CM} phenotype [45]. However, in our study, T_{EMRA} cells turned out to be the dominant population in both $CD4^+$ and $CD8^+$ subsets on day 7 before coculture. It might be attributed to several reasons, such as tonic signaling, specific scFv construct, or over-stimulation of CD3/CD28 beads. We tried to separate the beads at different times during the culture, but we did not find significant or profound changes regarding their differentiation. We are currently investigating this phenomenon further to better understand the underlying mechanisms.

When cocultured with Molm 13-WT cells, CD33 CAR-T cells secreted astonishing amount of IL-2, whereas Loop33×123 CAR-T cells had lower levels of secretion, but the proportion of residual target cells and CAR-T cell proliferation did not reveal significant differences between two groups. In addition, there were no variations concerning IL-6 secretion or other vital cytokines. Taken together, we showed that Loop33×123 CAR-T cells could effectively eliminate tumor cells while reducing IL-2 secretion. Elevated IL-2 secretion could be a strong indicator of T cell activation and proliferation [46], but excessive amount of cytokine could also trigger cytokine signaling cascade into cytokine release syndrome (CRS) [47]. In a recent clinical trial with CAR-T cells targeting CD33, [48] CRS occurred in 8 out of 9 patients (3 grade I, 3 grade II, and 2 grade III), which reminded us to be more cautious of cytokine secretion. We could not observe the same process in immunodeficient murine models; however, it was still an intriguing phenomenon that cytokine secretion ability might not be constantly correlated with cytotoxicity of CAR-T cells.

We speculated that both Loop33×123 and Loop123×33 CAR-T cells could significantly prolong mice survival, according to their relatively equivalent performances in vitro, but it was to our surprise that Loop123×33 CAR-T

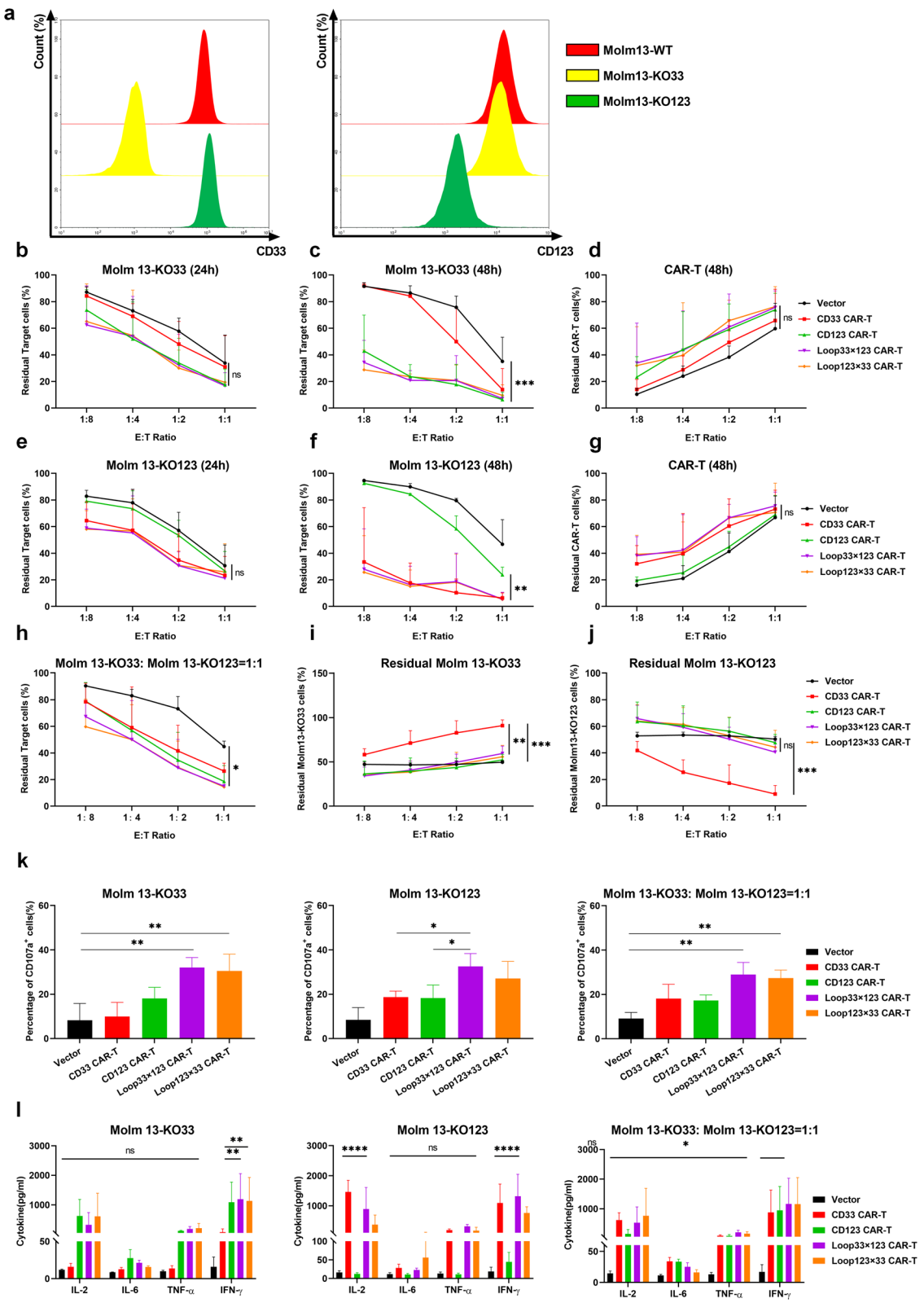

cells failed to show similar efficacy in vivo. Due to similar phenotypes and in vitro killing functions of Loop33×123 and Loop123×33 CAR-T cells, it might require in-depth sequencing to explore the underneath mechanism. In addition, we assumed that the different conformation of antigen recognition domains of these two CARs could change their

◂**Fig. 5** Loop33 × 123 CAR-T cells were efficient to avoid immune escape in vitro **a** FCM shows CD33 and CD123 expression on Molm 13-WT, Molm 13-KO33, and Molm 13-KO123. **b**–**d** Percentage of residual target cells and CAR-T cells at indicated time points after Vector-T or CAR-T cells were cocultured with Molm 13-KO33 cells at various E:T ratios. **e**–**g** Percentage of residual target cells and CAR-T cells at indicated time points after Vector-T or CAR-T cells were cocultured with Molm 13-KO123 cells at various E:T ratios. **h**–**j** Percentage of total residual target cells, percentage of residual Molm 13-KO33, and percentage of residual Molm 13-KO123 at 48 h after Vector-T or CAR-T cells were cocultured with a 1:1 mixture of Molm 13-KO33 and Molm 13-KO123 cells at various E:T ratios. **k** Degranulation of Vector-T or CAR-T cells defined as $CD107a^+$ cells after coculturing with Molm 13-KO33, Molm 13-KO123, or a 1:1 mixture of Molm 13-KO33 and Molm 13-KO123 cells for 6 h. **l** IL-2, IL-6, TNF-α, and IFN-γ secretion of Vector-T or CAR-T cells after coculturing with Molm 13-KO33, Molm 13-KO123, or a 1:1 mixture of Molm 13-KO33 and Molm 13-KO123 cells for 24 h. *, $p < 0.05$; **, $p < 0.01$; ***, $p < 0.001$; ****, $p < 0.0001$; ns, no significance

recognition ability, thus impacting the formation of immune synapse. To this point, we used computational programs to simulate the interaction between the scFv and the antigen. However, no significant differences were found. We are currently investigating into the immune synapse for better understanding of this phenomenon.

In the immune evasive models, we subjected CAR-T cells to Molm 13-KO33, Molm 13-KO123, or a mixture of both cell lines. While monovalent CAR-T failed to induce cytotoxicity, Loop CAR-T demonstrated reliable outcomes. However, CD123 CAR-T showed similar unbiased cytotoxicity in the mixture system, where both of tumor cell lines were equally eliminated, raising concerns about its off-target side effects. One possible reason for this phenomenon could be antigen spreading, which is a phenomenon in immunology where the immune response expands beyond the original target antigen to recognize and attack additional antigens [49]. In order to test this hypothesis, we cocultured CD123 CAR-T with Molm 13-KO33 first, and after 24 h, we sorted out CAR-T cells and coculture them with Molm 13-KO123. Surprisingly, CD123 CAR-T showed cytotoxicity toward Molm 13-KO123 cells, which was not observed before. In addition, we would investigate other possibilities in our future work, such as TCR repertoire and the identification of tumor antigen-specific T cell other than CAR-T cells.

Overall, our study demonstrated that Loop33 × 123 could efficiently eradicate AML cells while reducing the risks of antigen escape, which could be a possible dual targeting strategy applied to clinical practice.

Limitations

In this study, we chose to adjust CAR expression to 30% of all groups on day 7 instead of sorting CAR-T cells before coculture assays, which might cause unexpected bias in the following experiments. In addition, we did not thoroughly investigate the in vivo incapability of Loop123 × 33 CAR-T cells. We would keep investigating these issues in our future study.

Conclusion

Loop33 × 123 CAR-T targeting CD33 and CD123 could efficiently eliminate AML cells and prolong survival of tumor-bearing mice, while addressing the issue of immune escape. The engineered Loop33 × 123 CAR-T cells were a promising strategy to enhance the therapeutic intervention for AML.

Materials and methods

Cell lines and primary cells from AML patients

Human AML cell line Molm 13 and MV4-11 were cultured in RPMI-1640 medium supplemented with 10% fetal bovine serum (FBS). All leukemia cell lines, obtained from the American Type Culture Collection (ATCC), were grown at cell densities of $0.5–1 \times 10^6$ cells/ml and incubated at 37℃ with 5% CO_2 and high humidity.

To generate a CD33 and/or CD123 knockout Molm 13 cell line, the CRISPR-Cas9 technology was employed. Two guide RNAs were employed: 5'-ATCCCTGGC ACTCTAGAACC-3'; 5'-GACCAACTACACCGTCCG AG-3'. The guide RNA was cloned into the lenti CRISPRv2 plasmid (Addgene, plasmid #52,961). Molm 13 cells were transfected with lentivirus. $CD33^+$ $CD123^-$ (Molm 13-KO123), $CD33^-$ $CD123^+$ (Molm 13-KO33), and $CD33^-$ $CD123^-$ (Molm 13-KO33&123) clones were sorted through flow cytometry (BD, FACSAria III) and subsequently cultured.

Bone marrow samples were obtained from primary AML patients who were enrolled in the Institute of Hematology & Blood Diseases Hospital, Chinese Academy of Medical Sciences & Peking Union Medical College (CAMS & PUMC), and the informed consents were signed. These cells were cultured in IMDM supplemented with 15% FBS, 100 ng/ml recombinant human Fms-like tyrosine kinase 3 ligand (rhFLT3-L, PEPROTECH, Cat.#300–19), 100 ng/ml recombinant human stem cell factor (rhSCF, PEPROTECH, Cat.#300–17), and 50 ng/ml recombinant human thrombopoietin (rhTPO, PEPROTECH, Cat.#300–18).

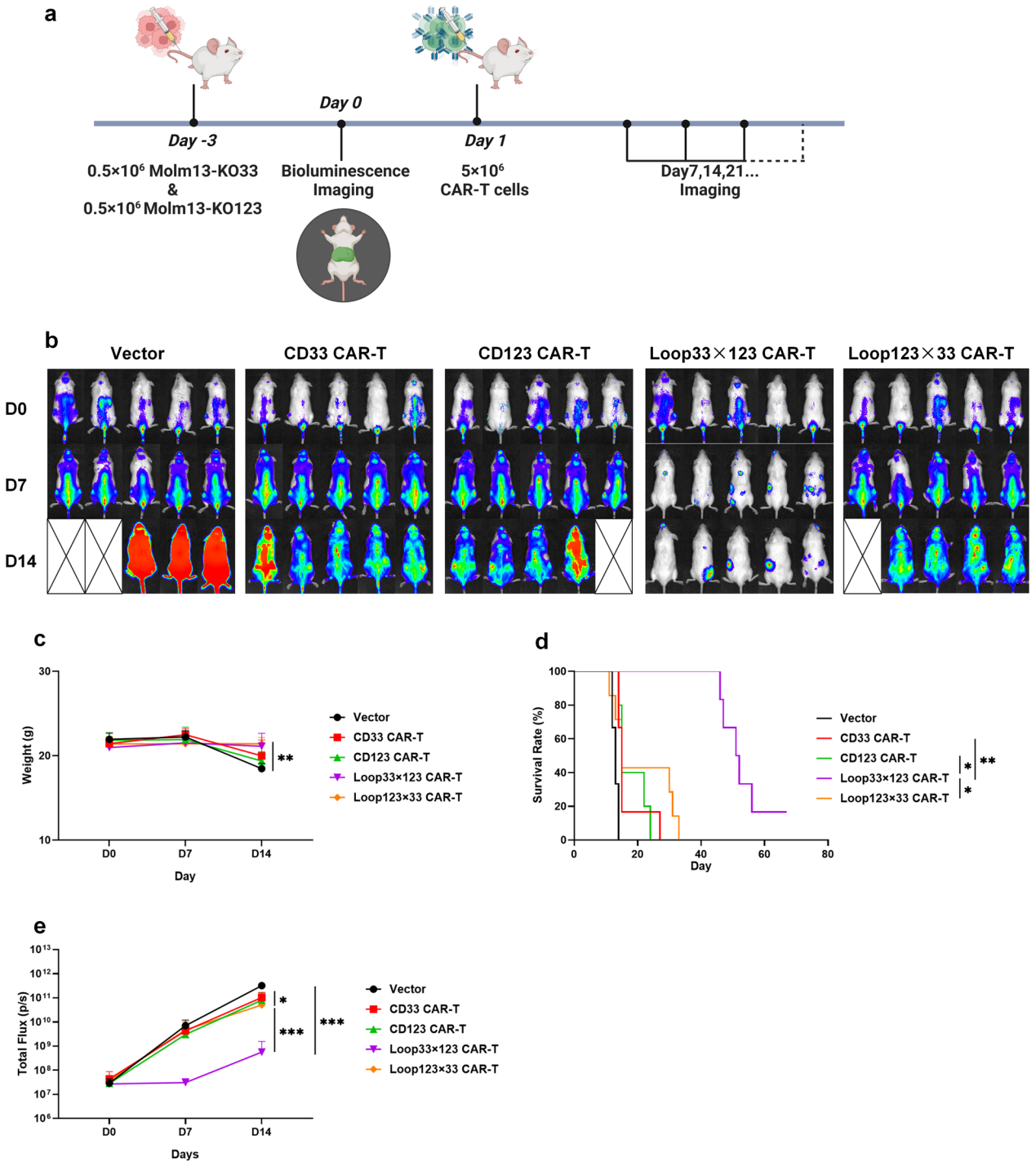

Fig. 6 Loop33×123 CAR-T cells were efficient to avoid immune escape in vivo **a** The experimental regimen of the B-NDG-CDX model. **b** Bioluminescence imaging showing tumor burden at indicated time ($n=5$). **c** The body weight of each group was measured after treatment with Vector-T or CAR-T cells. **d** Kaplan–Meier survival curves for each group. **e** Statistical analysis of the bioluminescence intensity. *, $p<0.05$; **, $p<0.01$; ***, $p<0.001$; ****, $p<0.0001$; ns, no significance

Viral constructs

Lentivirus vectors were constructed using the pCDH-EF1α backbone. The CD33-targeted single-chain variable fragment (scFv) and CD123-targeted scFv were derived from the respective monoclonal antibody hybridoma clones HIM3-4/HI33a and 13C3 in our previous studies [34]. These

sequences were connected with different linkers. Coding sequences were as follows:

Linker1:GGTGGCGGTGGCTCGGGTGGAGGTGGATCTGGTGGTGGCGGTTCG.

Linker2:GGTGGTGGTGGTTCT.

Linker3:GGAAGTACAAGCGGTAGCGGAAAACCCGGCTCTGGAGAAGGATCAACAAAAGGT.

These scFv were followed with CD8 hinge and transmembrane domain, 4-1BB, and CD3ζ signaling domains. Lentivirus production was carried out using HEK293T cells. Viral supernatants were purified through precipitation with PEG-8000 and NaCl. The resulting viral pellet was resuspended in KBM581 (Corning, USA) for human T cell infection.

Generation of car-T cells

Human $CD3^+$ T cells were isolated from healthy donors from Tianjin Blood Center using the human T Cells Enrichment Cocktail (STEMCELL, USA, Cat.# 15,021) following the manufacturer's protocol. To generate CAR-T cells, T cells were activated on day 0 using CD3/CD28 Dynabeads (Gibco, Cat.# 11131D) and cultured in lymphocyte medium KBM581 (Corning, USA) supplemented with 5% FBS and 50 IU/mL recombinant human IL-2 (RD Systems, USA, Cat.# 200IL-500). On day 1, T cells were transduced with lentiviral supernatants. On day 7, transduction efficiency was determined using FCM (Agilent, NovoCyte) with PE-labeled CD33 protein (AcroBIOSYSTEMS, Cat.# CD3-HP2E3) and APC-labeled CD123 protein (AcroBIOSYSTEMS, Cat.# ILA-HA2H8).

T cell phenotyping

The analysis of CAR-T cell phenotypes was conducted using FCM, focusing on activation and proliferation markers: CD69 and CD25 expression. Additionally, the percentages of $Tim3^+$, $Lag3^+$, and $PD\text{-}1^+$ cells were evaluated, along with the memory markers CD45RA and CCR7.

Cytotoxicity assays

CAR-T cells were incubated with tumor targets at different effector to target (E:T) ratios in KBM581 supplemented with 5% FBS without rhIL-2.

Effector cells and target cells were seeded at various E:T ratio, specifically 1:8, 1:4, 1:2, and 1:1 in a 24-well plate. The percentage of residual target cells was determined using FCM at 24 and 48 h. Residual cells were defined as followed: $CD3^+$ T cells, $CD3^-$ $CD33^+$ Molm 13-WT, $CD3^-$ Molm 13-KO33&123, $CD3^-$ $CD33^-$ $CD123^+$ Molm 13-KO33, and $CD3^-$ $CD33^+$ $CD123^-$ Molm 13-KO123.

Degranulation assay

CAR-T cells were incubated with target cells at an E:T ratio of 1:1 in a 96-well plate supplemented with 100 IU/mL IL-2, anti-human CD107a antibody (H4A3). After 1 h, 2 μM Monensin (Biolegend, USA, Cat.# 420,701) was added. After 6 h of co-culture, the percentage of $CD107a^+$ T cells was analyzed using FCM.

Detection of cytokine release

The co-culture supernatant from the specific killing assay at an E:T ratio of 1:1 was collected. The concentrations of interleukin 2 (IL-2), interleukin 6 (IL-6), interferon-gamma (IFN-γ), and tumor necrosis factor-alpha (TNF-α) were quantified by the capture of microspheres encapsulated with cytokine-specific antibodies (Cellgene Biotech, China, Cat.#P420487) using FCM.

In vivo experiments

Six-week-old female NOD.CB17-$Prkdc^{scid}Il2rg^{tm1Bcgen}$/Bcgen (B-NDG, BIOCYTOGEN, Cat.# 110,586) mice were used with the approval of the Institutional Animal Care and Use Committee of Peking Union Medical College. Mice were administered intravenous injections of 1×10^6 Molm13-luciferase cells, engineered in our laboratory through the transfection of Molm 13 cells with luciferase, on day 3. They were randomly assigned to five groups based on their weights and bioluminescence intensity on day 0. On day 1, mice received intravenous administration of 5×10^6 Vector-T or CAR-T cells. Mice body weights were monitored weekly. For dynamic tumor burden monitoring, mice were intraperitoneally anesthetized with avertin, infused with D-luciferin (150 mg/kg body weight, Yeason, Cat.# 40902ES01), and subjected to weekly bioluminescence imaging using Caliper IVIS Lumina II (Caliper Life Sciences, USA). Overall survival time was recorded.

Statistical analysis

The statistical analysis of the data was performed using GraphPad Prism 8.0. Data were presented as mean ± SEM. A two-tailed Student's t test was applied to compare parametrically distributed variables between two groups. For analyses involving three or more groups, a two-way ANOVA with Tukey's multiple comparison test was employed. The Kaplan–Meier technique was used to estimate overall survival. Log-rank (Mantel- Cox) test was used to assess

differences. Statistical significance is indicated by the symbols: *, $p < 0.05$; **, $p < 0.01$; ***, $p < 0.001$; ****, $p < 0.0001$; ns, no significance.

Supplementary Information The online version contains supplementary material available at https://doi.org/10.1007/s00262-024-03847-7.

Author contributions HM and ZY wrote the main manuscript text and contributed to analysis and interpretation of results. RG, YX, SQ, HX, KT, ZT, and QR contributed to conception and design of this work. MW and JW rewrote the manuscript and approved the final accepted version of the manuscript.

Funding This work was supported by the National Key Research & Development Program of China (2021YFC2500300), the National Natural Science Foundation of China (82341213), and the CAMS Innovation Fund for Medical Sciences (2021-I2M-1-041).

Data availability Data are provided within the manuscript or supplementary information files.

Declarations

Conflict of interest The authors declare no competing interests.

References

1. Siegel RL, Miller KD, Wagle NS, Jemal A (2023) Cancer statistics, 2023. CA A Cancer J Clinic 73(1):17–48. https://doi.org/10.3322/caac.21763
2. Short NJ, Konopleva M, Kadia TM, Borthakur G, Ravandi F, DiNardo CD et al (2020) Advances in the treatment of acute myeloid leukemia: new drugs and new challenges. Cancer Discov 10(4):506–525
3. June CH, O'Connor RS, Kawalekar OU, Ghassemi S, Milone MC (2018) CAR T cell immunotherapy for human cancer. Science (New York, NY) 359(6382):1361–1365
4. Ying Z, Huang XF, Xiang X, Liu Y, Kang X, Song Y et al (2019) A safe and potent anti-CD19 CAR T cell therapy. Nat Med 25(6):947–953
5. Liu H (2021) Emerging agents and regimens for AML. J Hematol Oncol 14(1):49
6. Bäumer N, Scheller A, Wittmann L, Faust A, Apel M, Nimmagadda SC et al (2022) Electrostatic anti-CD33-antibody-protamine nanocarriers as platform for a targeted treatment of acute myeloid leukemia. J Hematol Oncol 15(1):171
7. Kenderian SS, Ruella M, Shestova O, Klichinsky M, Aikawa V, Morrissette JJ et al (2015) CD33-specific chimeric antigen receptor T cells exhibit potent preclinical activity against human acute myeloid leukemia. Leukemia 29(8):1637–1647
8. Petty NE, Radtke S, Fields E, Humbert O, Llewellyn MJ, Laszlo GS et al (2023) Efficient long-term multilineage engraftment of CD33-edited hematopoietic stem/progenitor cells in nonhuman primates. Molecul Therap Method Clinic Developm 31:101121
9. Laszlo GS, Harrington KH, Gudgeon CJ, Beddoe ME, Fitzgibbon MP, Ries RE et al (2016) Expression and functional characterization of CD33 transcript variants in human acute myeloid leukemia. Oncotarget 7(28):43281–43294
10. O'Hear C, Heiber JF, Schubert I, Fey G, Geiger TL (2015) Anti-CD33 chimeric antigen receptor targeting of acute myeloid leukemia. Haematologica 100(3):336–344
11. Molica M, Perrone S, Mazzone C, Niscola P, Cesini L, Abruzzese E, de Fabritiis P (2021) CD33 Expression and gentuzumab ozogamicin in acute myeloid leukemia: two sides of the same coin. Cancers 13(13):3214. https://doi.org/10.3390/cancers13133214
12. Wang QS, Wang Y, Lv HY, Han QW, Fan H, Guo B et al (2015) Treatment of CD33-directed chimeric antigen receptor-modified T cells in one patient with relapsed and refractory acute myeloid leukemia. Molecul Therap J Am Soc Gene Therap 23(1):184–191
13. Caruso S, De Angelis B, Del Bufalo F, Ciccone R, Donsante S, Volpe G et al (2022) Safe and effective off-the-shelf immunotherapy based on CAR.CD123-NK cells for the treatment of acute myeloid leukaemia. J Hematol Oncol 15(1):163
14. Tabata R, Chi S, Yuda J, Minami Y (2021) Emerging immunotherapy for acute myeloid leukemia. Int J Molecul Sci 22(4):1944. https://doi.org/10.3390/ijms22041944
15. Lamble AJ, Eidenschink Brodersen L, Alonzo TA, Wang J, Pardo L, Sung L et al (2022) CD123 expression is associated with high-risk disease characteristics in childhood acute myeloid leukemia: a report from the children's oncology group. J Clinical Oncol Off J Am Soc Clinical Oncol 40(3):252–261
16. Al-Mawali A, Gillis D, Lewis I (2016) Immunoprofiling of leukemic stem cells CD34+/CD38-/CD123+ delineate FLT3/ITD-positive clones. J Hematol Oncol 9(1):61
17. Herrmann H, Sadovnik I, Eisenwort G, Rülicke T, Blatt K, Herndlhofer S et al (2020) Delineation of target expression profiles in CD34+/CD38- and CD34+/CD38+ stem and progenitor cells in AML and CML. Blood Adv 4(20):5118–5132
18. Ehninger A, Kramer M, Röllig C, Thiede C, Bornhäuser M, von Bonin M et al (2014) Distribution and levels of cell surface expression of CD33 and CD123 in acute myeloid leukemia. Blood Cancer J 4(6):e218
19. Han YC, Kahler J, Piché-Nicholas N, Hu W, Thibault S, Jiang F et al (2021) Development of highly optimized antibody-drug conjugates against CD33 and CD123 for acute myeloid leukemia. Clinical Cancer Res An Off J Am Assoc Cancer Res 27(2):622–631
20. Albinger N, Pfeifer R, Nitsche M, Mertlitz S, Campe J, Stein K et al (2022) Primary CD33-targeting CAR-NK cells for the treatment of acute myeloid leukemia. Blood Cancer J 12(4):61
21. Baroni ML, Martinez DS, Aguera FG, Ho HR, Castella M, Zanetti SR, Hernandez TV, Diaz R, de la Guardia J, Castaño EA, Vives S, Nomdedeu J, Lapillone H, Bras AE, van der Velden VHJ, Junca J, Marin P, Bataller A, Esteve J, Vick B, Jeremias I, Lopez A, Sorigue M, Bueno C, Menendez P (2020) 41BB-based and CD28-based CD123-redirected T-cells ablate human normal hematopoiesis in vivo. J Immuno Therap Cancer 8(1):e000845. https://doi.org/10.1136/jitc-2020-000845
22. Li H, Xu S, Quan J, Yung BC, Pang J, Zhou C et al (2015) CD33-Targeted lipid nanoparticles (aCD33LNs) for therapeutic

delivery of GTI-2040 to acute myelogenous leukemia. Mol Pharm 12(6):2010–2018
23. Pizzitola I, Anjos-Afonso F, Rouault-Pierre K, Lassailly F, Tettamanti S, Spinelli O et al (2014) Chimeric antigen receptors against CD33/CD123 antigens efficiently target primary acute myeloid leukemia cells in vivo. Leukemia 28(8):1596–1605
24. Atilla PA, McKenna MK, Watanabe N, Mamonkin M, Brenner MK, Atilla E (2022) Combinatorial antigen targeting strategies for acute leukemia: application in myeloid malignancy. Cytotherapy 24(3):282–290
25. Sun S, Zou H, Li L, Liu Q, Ding N, Zeng L et al (2019) CD123/CD33 dual-antibody modified liposomes effectively target acute myeloid leukemia cells and reduce antigen-negative escape. Int J Pharm 568:118518
26. Liu S, Deng B, Yin Z, Lin Y, An L, Liu D et al (2021) Combination of CD19 and CD22 CAR-T cell therapy in relapsed B-cell acute lymphoblastic leukemia after allogeneic transplantation. Am J Hematol 96(6):671–679
27. Zhang Y, Li S, Wang Y, Lu Y, Xu Y, Rao Q, Wang H, Xing H, Tian Z, Tang K, Lv L (2022) A novel and efficient CD22 CAR-T therapy induced a robust antitumor effect in relapsed/refractory leukemia patients when combined with CD19 CAR-T treatment as a sequential therapy. Experimen Hematol Oncol 11(1):15
28. Tong C, Zhang Y, Liu Y, Ji X, Zhang W, Guo Y et al (2020) Optimized tandem CD19/CD20 CAR-engineered T cells in refractory/relapsed B-cell lymphoma. Blood 136(14):1632–1644
29. Yang M, Tang X, Zhang Z, Gu L, Wei H, Zhao S et al (2020) Tandem CAR-T cells targeting CD70 and B7–H3 exhibit potent preclinical activity against multiple solid tumors. Theranostics 10(17):7622–7634
30. Petrov JC, Wada M, Pinz KG, Yan LE, Chen KH, Shuai X et al (2018) Compound CAR T-cells as a double-pronged approach for treating acute myeloid leukemia. Leukemia 32(6):1317–1326
31. Wang Z, Lu Y, Liu Y, Mou J, Liu X, Chen M et al (2023) Novel CD123×CD33 bicistronic chimeric antigen receptor (CAR)-T therapy has potential to reduce escape from single-target CAR-T with no more hematotoxicity. Cancer Commun (London, England) 43(10):1178–1182
32. Chen Z, Liu Y, Chen N, Xing H, Tian Z, Tang K et al (2023) Loop CD20/CD19 CAR-T cells eradicate B-cell malignancies efficiently. Sci China Life Sci 66(4):754–770
33. Li S, Tao Z, Xu Y, Liu J, An N, Wang Y, Xing H, Tian Z, Tang K, Liao X, Rao Q, Wang M, Wang J (2018) CD33-specific chimeric antigen receptor T cells with different Co-stimulators showed potent anti-leukemia efficacy and different phenotype. Hum Gene Ther 29(5):626–639
34. Gorczyca W, Sun ZY, Cronin W, Li X, Mau S, Tugulea S (2011) Immunophenotypic pattern of myeloid populations by flow cytometry analysis. Method Cell Biol 103:221–266. https://doi.org/10.1016/B978-0-12-385493-3.00010-3
35. Arndt C, von Bonin M, Cartellieri M et al (2013) Redirection of T cells with a first fully humanized bispecific CD33-CD3 antibody efficiently eliminates AML blasts without harming hematopoietic stem cells. Leukemia 27(4):964–967
36. Pollard JA, Guest E, Alonzo TA et al (2021) Gemtuzumab ozogamicin improves event-free survival and reduces relapse in pediatric KMT2A-rearranged AML: results from the phase iii children's oncology group Trial AAML0531. J Clin Oncol 39(28):3149–3160
37. Schlenk RF, Paschka P, Krzykalla J et al (2020) gemtuzumab ozogamicin in NPM1-mutated acute myeloid leukemia: early results from the prospective randomized AMLSG 09–09 phase III study. J Clin Oncol 38(6):623–632
38. Daver NG, Montesinos P, DeAngelo DJ et al (2024) Pivekimab sunirine (IMGN632), a novel CD123-targeting antibody-drug conjugate, in relapsed or refractory acute myeloid leukaemia: a phase 1/2 study. Lancet Oncol 25(3):388–399
39. Al-Hussaini M, Rettig MP, Ritchey JK et al (2016) Targeting CD123 in acute myeloid leukemia using a T-cell-directed dual-affinity retargeting platform. Blood 127(1):122–131
40. Jin X, Xie D, Sun R, Lu W, Xiao X, Yu Y et al (2023) CAR-T cells dual-target CD123 and NKG2DLs to eradicate AML cells and selectively target immunosuppressive cells. Oncoimmunology 12(1):2248826
41. John S, Chen H, Deng M, Gui X, Wu G, Chen W et al (2018) A Novel Anti-LILRB4 CAR-T cell for the treatment of monocytic AML. Molecul Therap J Am Soc Gene Therap 26(10):2487–2495
42. Meyer JE, Loff S, Dietrich J, Spehr J, Jurado Jiménez G, von Bonin M et al (2021) Evaluation of switch-mediated costimulation in trans on universal CAR-T cells (UniCAR) targeting CD123-positive AML. Oncoimmunology 10(1):1945804
43. Chevallier P, Robillard N, Ayari S, Guillaume T, Delaunay J, Mechinaud F et al (2008) Persistence of CD33 expression at relapse in CD33(+) acute myeloid leukaemia patients after receiving Gemtuzumab in the course of the disease. Br J Haematol 143(5):744–746
44. Wang QS, Wang Y, Lv HY et al (2015) Treatment of CD33-directed chimeric antigen receptor-modified T cells in one patient with relapsed and refractory acute myeloid leukemia. Mol Ther 23(1):184–191. https://doi.org/10.1038/mt.2014.164
45. Bulliard Y, Andersson BS, Baysal MA, Damiano J, Tsimberidou AM (2023) Reprogramming T cell differentiation and exhaustion in CAR-T cell therapy. J Hematol Oncol 16(1):108
46. Boyman O, Sprent J (2012) The role of interleukin-2 during homeostasis and activation of the immune system. Nature Rev Immunol 12(3):180–190
47. Morris EC, Neelapu SS, Giavridis T, Sadelain M (2022) Cytokine release syndrome and associated neurotoxicity in cancer immunotherapy. Nat Rev Immunol 22(2):85–96
48. Liu F, Cao Y, Pinz K, Ma Y, Wada M, Chen K, Ma G, Shen J, Tse CO, Su Y, Xiong Y (2018) First-in-human CLL1-CD33 compound CAR T cell therapy induces complete remission in patients with refractory acute myeloid leukemia: update on phase 1 clinical trial. Blood 29(132):901
49. Brossart P (2020) The Role of Antigen Spreading in the Efficacy of Immunotherapies. Clin Cancer Res 26(17):4442–4447